International Physicists' Tournament

Preselection Report

Problem 4 – Travelling Flames

January 2025

I. INTRODUCTION

Under certain circumstances a flame can travel along an open canal (see link below). Explain the phenomenon. Investigate its lifetime and speed. Under which circumstances does it display a periodic behavior? Maximize the lifetime of a traveling flame for a given amount of fuel.

Combustion is a rapid oxidation process in which a combustible material reacts, often with the oxygen in the air, releasing heat and light [14]. For many reactions, such as wood fires, the energy change from the reaction exceeds the activation energy, enabling the material to sustain combustion until the fuel is depleted. The release of energy in the form of heat and expanding gases under constant pressure is characterized by enthalpy. The three essential components for combustion—commonly depicted in the "fire triangle"—are an oxidizer (typically oxygen in the air), a fuel source, and a consistent source of heat to sustain the reaction.

When liquid fuels such as gasoline, naphtha, or alcohol are used, they evaporate to release highly flammable fumes. If a puddle of such fuel is ignited, it can cause a violent explosion and sustain combustion in an open environment. However, when the fuel is partially encased in a ring structure, the limited oxygen supply creates conditions where combustion cannot be sustained for long before the oxygen gets depleted. In this setup, if the vapors are ignited by a lighter, small flames are produced that travel around the ring. The flame propagates by igniting vapor ahead of it while extinguishing the fuel behind it, provided there is sufficient fuel vapor and oxygen to sustain the reaction.

When the hydrocarbon vapor above the ring is ignited, the heat triggers a combustion reaction between the fuel vapor and the oxygen. The flame often separates and travels in opposite directions. If only one side is initially lit, the flame propagates continuously around the ring for a limited duration, determined by factors such as the ring's size, the fuel used, and the oxygen flow through the channels.

In this configuration, fuel evaporates within the channels and mixes with the surrounding oxygen. Ignition occurs when a lighter supplies sufficient heat to initiate combustion. However, the reaction can only take place if the fuel vapor concentration is within the fuel's flammability range—between the lower explosive limit (LEL) and the upper explosive limit (UEL). Too little or too much vapor will prevent ignition [8].

Once the vapor is ignited, the thermal energy of the flame transfers to adjacent, cooler vapor layers through thermal conduction, triggering combustion in the neighboring fuel molecules. This produces new flames on either side of the original flame, which propagate as the reaction consumes unburnt vapor. When the vapor is depleted, that part of the flame extinguishes, creating a tail of cooling gases. Eventually, the flames meet at the opposite side of the ring, where no further fuel vapor remains, causing the combustion to cease.

If one side of the ring is covered during ignition, the oxygen and heat supply are blocked on that side, preventing combustion there and allowing a flame to form only on the uncovered side. This flame will travel around the ring until it returns to its starting point. If sufficient time has passed for fuel vapor to accumulate above the lower explosive limit during the refractory period, the flame can ignite the vapor again and continue traveling around the ring. This cyclical process depends on the balance between fuel evaporation and oxygen availability.

II. THEORETICAL MODELING

To understand how we can predict the velocity and lifetime of the flame as it propagates through the channels, various characteristic properties of the gas need to be known. Namely, the thermal conductivity, specific heat capacity, density, rate of evaporation and temperature. These can be considered as the physical properties of the fuel. It must be noted, however, that because this is a combustion reaction, these same properties need to be accounted for the atmosphere in which the reaction is taking place, namely ambient air.

Furthermore, given that this is a combustion reaction after all, there are certain chemical properties that need to be considered as well. Namely, for a chemical reaction of the form $n\text{Fuel} + m\text{Oxidizer} \rightarrow \text{Products}$, the activation energy of this reaction as well as the flame temperature and ignition temperature (minimal temperature at which the fuel needs to reach to ignite) need to be known. Knowing all of these parameters, we can finally find the laminar flame speed, S_L as seen in Equation 1.

A. Dynamics and Velocity of Flame Propagation

To understand how the flame propagates, we will need to make a few assumptions. First, the flame front is laminar, which means the gases near the front all behave uniformally. In other words, neighboring regions of the front all travel in a smiliar direction and speed. Furthermore, the unburned gases ahead of the front are quiescent, meaning that they do not have any significant velocities in the first place. Furthermore, because the gas itself is not enclosed in a container, they are subject to constant pressure, in this case, near atmospheric pressure (approximately 100.9 kPa).

$$S_L = \sqrt{\alpha\dot{\omega}\frac{T_B - T_i}{T_i - T_u}} \tag{1}$$

$$\dot{\omega} = Ae^{\frac{-E_a}{k_b T}}[F]^n[O]^m \tag{2}$$

, where α is the thermal diffusion constant of the fuel-air mixture, $\dot{\omega}$ is the reaction rate and T_B, T_i and T_u are the burned, ignition and unburned fuel temperatures [15]. For the reaction rate, A is a pre-exponential factor that determines the reaction rate, E_a again is the activation energy, k_b is Boltzmann's constant, T is the temperature in Kelvin, [F] is the concentration of fuel molecules and [O] is the concentration of the oxidizer molecules in the mix and n/m are the empirically found partial orders of the reaction. For the oxidizer concentration, we assumed the concentration of oxygen in the air inside the channels to be approximately 10%.

Finally, by taking a look at Equation 2, we can make the reasonable assumption that the rate of the reaction $\dot{\omega}$ is related to the temperature via the Arrhenius equation [12], as shown in Equation 3. Similarly, we can also assume that this reaction rate is dependent on the to the amount usable reactants still available, namely that $\dot{\omega} = -B\omega$, thus giving Equation 4.

$$k = Ce^{-\frac{E_a}{k_b t}} \tag{3}$$

$$\omega = De^{-Bt} \tag{4}$$

Here, k is the frequency of collisions between reactant atoms, k_b is Boltzmann's constant and t is time. For the second equation, D is a constant relating to the initial quantity of unreacted gas before combustion takes place and B defines the characteristic rate of combustion.

To consolidate the fact that the reaction rate requires the physical parameters to account for a mixture of air and fuel, the concentration of both are required. To do so, the rate of the fuel's evaporation and the air's rate of diffusion into the channel need to be found. Although the former is easy to measure, the latter is much harder to estimate. That said, it can be deduced through various runs since this rate should be the same for any given geometry, no matter the fuel. As such, given enough experiments, this rate of diffusion can be found by measuring the velocity of propagation for various fuels. Furthermore, it should be noted that this rate is assumed to be linearly proportional to the area of the channel's opening.

In this, by finding this diffusion parameter, the concentration of oxygen in the channel with respect to time can be found. By searching for the fuel's rate of evaporation, pre-exponential factor and activation energy, the reaction rate, and therefore propagation velocity, may be found.

B. Lifetime of the Flame

Lastly, there are two factors that will decide the lifetime of the flame. Firstly is the evaporation of the fuel. Given that the channels have rather small openings which restrict airflow, fuels tend to be of high volatility. In other words, their rates of evaporation are high. As such, even in the absence of a flame, the fuel will slowly dissipate into the air. Although not a perfect model, we can assume that changes in temperature follow a Newtonian model, namely [10]:

$$\frac{dQ}{dt} = A \cdot h\Delta T \tag{5}$$

$$M(T) = \Gamma(298) \cdot \sigma(T) \cdot t \cdot A \tag{6}$$

$$T(x) = T_b e^{-\gamma x} + T_0 \tag{7}$$

, where $\frac{dQ}{dt}$ is the change in energy due to loss of heat, h is the heat transfer coefficient, A is the area of contact and Δ T is the difference in temperature between the two neighboring sides. Equation 6 predicts the mass of evaporated fuel $M(T)$, where $\Gamma(298)$ is the evaporation rate at room temperature, t is time and A is the surface area of the opening of the channel. As can be checked in Equation 9 in the annexe, the references for evaporation rate were measured at 298K. As such, given that our fuels experience varying temperatures over time, we need to introduce an additional factor to compensate. This factor, $\sigma(T)$ compensates the disparity by calculating the portion of molecules in a substance at 298K that exceed the energy required to evaporate (enthalpy of vaporization). Then, by comparing that to the portion of molecules that exceed this limit at a higher temperature (or in this case, a temperature distribution across the length of the channel), we get σ, which behaves as a factor increasing the evaporation rate. To calculate these portions, we integrate Boltzmann distributions for each fuel are calculated from the enthalpy required to evaporate that fuel to infinity. In this case, we believe that the temperature profile will follow an exponentially decaying curve as shown in equation 7, where $T(x)$ is the temperature of the fuel across the channel length, T_b is the temperature of the flame, γ is the decay rate of the flame over distance and T_0 the minimum temperature of the channel.

This similarly follows an exponential behaviour as the above equations. Crucially, this means that when the difference in temperature is high, so is the change in temperature; when the difference is low, so is the transfer. Furthermore, given that the PLA tracks behave as a heat sink and that the mass of the fuel is very small (on the order of 50mg), the thermal properties of the PLA play a crucial role and those of the fuel may be largely ignored.

In fact, it must be stated that the properties of the PLA does not directly influence the combustion as long as it does not react nor get dissolved by the solvents. This is the case for all fuels used except acetone (in which case, experiments were conducted quickly), where conclusions must be more conservative. As stated above however, the PLA tracks play a crucial role in the thermal properties of the experiments. If further theoretical calculations were to take place, the specific heat capacity, mass, geometries and heat conductivity of the PLA need to be considered. It should be noted that experiments were attempted with tracks covered in aluminum foil (as to prevent any direct plastic-to-solvent interactions), but the extra surface area resulted in explosive results. As such, a track machined out of aluminum will be used to test the thermal properties of the tracks further.

C. Length of the Flame

Because the distance we travel along the channel is proportional to some change in time, we can correlate distances behind the flame front to a past time when the reaction initially took place. As such, we should expect the flame's shape to approximately look like an exponentially decaying reaction area in space, as predicted by Newtonian cooling. In other words, the shape of the flame should behave as a sharp point where the flame starts, and a long tail which exponentially gets colder (and darker), as we move away from the center.

III. METHODOLOGIES

This experiment heavily relies on 3D printing to create the setups necessary to consider what parameters affect the flame shape, velocity and lifetime. As shown above, many of the parameters depend on the fuel's characteristic properties, so varying the channels may provide insight on the physical mechanisms behind the travelling flames.

A. Materials Used

By using parameterized files of the loop model offered in Steve Mould's video, we had the ability to easily vary several parameters. The radius of curvature of the rings as well as the angle of their opening were of particular interest, as shown in Figure 1. Longer rings should allow for the fuel to evaporate for longer. This should result in more heat generated per unit length of the ring and thus facilitate the flame to travel forward.

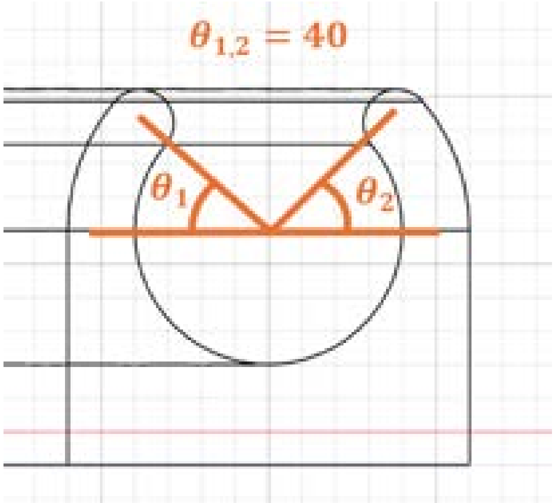

(a) Wireframe image from Fusion 360 showing how the angle parameter is defined. In this report, $\theta_1 = \theta_2$. That said, further experiments, will verify if a lopsided opening affects the dynamics of the flames.

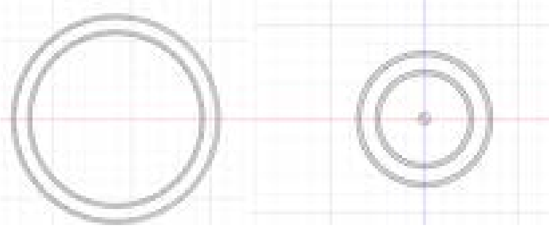

(b) Wireframe image from Fusion 360 showing how the radius parameter is defined. This parameter simply changes the radius of curvature over which the flame travels. Here, the radii are 6cm and 3cm respectively.

Fig. 1: Wireframe images from Fusion 360 of the various parameters used in the 3D models of the channels.

Once a model is created, the files are then 3D printed using PLA filament. For this report, five fuel sources were used, those being isopropyl alcohol, methanol, acetone, zippo lighter fluid (made of light petroleum distillates) as well as a water/methyl acetate mixture. Down the line, other fuel sources, like hexanes, benzene and long-chain hydrocarbons will be used as well.

As seen in Figure 2, by setting up a camera to take zoomed-in photos of the flame and a phone camera to capture slow-motion video, the experiment is now setup. Other equipment includes a lighter, a small syringe, various rings and a temperature sensor to find the temperature of the setups before and after burning the fuel. It is imperative to do these experiments in an area with good ventilation (to prevent any fumes from accumulating), tough this results in higher evaporation rates than usual. Furthermore, dim lighting must be used, as the light emitted by the flames is dim compared to sunlight or even LED lighting.

Fig. 2: Image of the setup used to make measurements. On the right is a DSLR camera (A) capable of shooting 1ms exposure. Next to the left is the 3D-printed channel (B). Above it is a syringe used to take out 0.1mL of fuel at a time (C). To the left of that is a lighter used to ignite the fuel (D). Finally, on the left is a temperature meter and thermocouple that were used to measure the temperature of the fuel after burning nearly to completion (E). On top (F), the fuels used are the methyl-acetate/water mixture, methanol, isopropyl alcohol, acetone and zippo lighter fluid. Not shown, the phone camera used to record slow motion video.

B. Experimentation and Analysis

Experiments were performed by first placing the phone near the ring and starting to record in slow-motion. Then, the syringe is used to measure out the fuel. In these experiments, 0.1mL of fuel was used per 37.7cm of track. The tracks are then quickly lifted and rotated such that the fuel evenly disperses across the channels. Then, the lights are dimmed and a finger is placed on the track, blocking access to air and to the fuel. The lighter is then brought to a piece of the track near the finger and lights the fuel. Two flames appear, but one dies out at the finger, while the other travels the other direction. Quickly, the finger is released.

The flame is allowed to circulate around the track until it dies and the recordings are stopped. If the whole channel catches on fire or the flame gets stuck on a piece of PLA, the trial is restarted. Each experiment runs three trials. Measuring the time between ignition and extinguishment yields the lifetime, whereas the number of laps completed by the flame times the ring's circumference divided by the lifetime yields the velocity.

For imaging the flame, a high focal ratio lens is used and the camera is set to its most sensitive gain. 1ms exposures are taken to minimize motion blur, and the image is analyzed using imageJ. Crucially, a line segment following the center of the flame is used to plot the brightness of each pixel along the flame. By isolating the peak brightness and smoothing each datum over 10 neighboring points (to minimize noise) an exponential decay may be observed and fitted.

IV. RESULTS

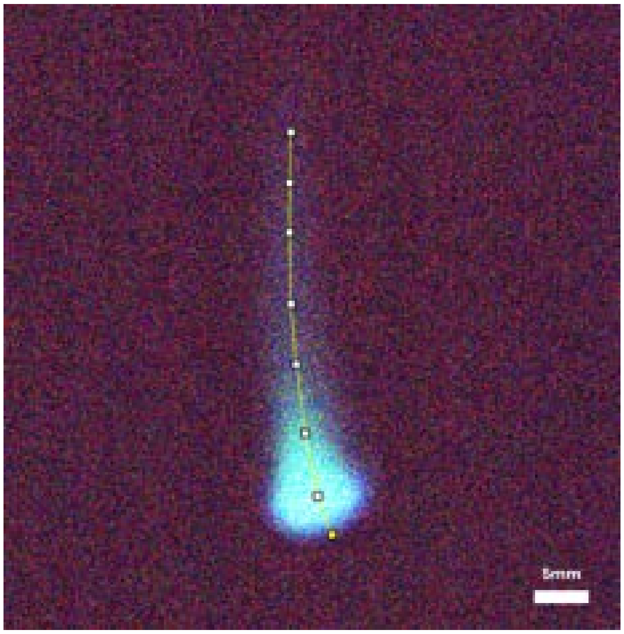

(a) A 0.001s exposure of a flame-burning Zippo lighter fuel. Overlayed is a segmented line along which the brightness of each pixel is measured. It should be noted that the flame is not a point, but rather has a long tail that gets exponentially darker.

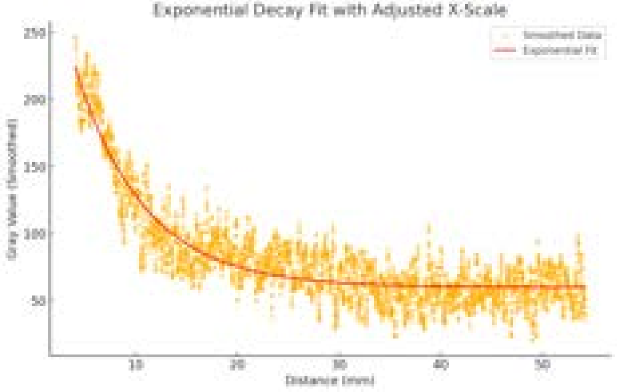

(b) Graph showing the brightness of the flame across its length on the segmented line shown above. Overlayed is a best-fit curve following an exponential decay. It can be seen that the flame brightness, and therefore temperature, follow an exponential decay over space.

Fig. 3: Image and graph of the brightness of a flame with respect to the distance behind its front. A similar graph is presented in the appendices, where Figure 7 demonstrates how various fuel (of significantly different chemical and physical properties) have largely the same flame profiles.

$$I \propto \sigma T^4 \tag{8}$$

It is important to note that Figure 3 purely plots the brightness of the flame. As such, to relate that to temperature, we must make the approximation that the flame burning is approximated by a black-body [13]. As such, if we carefully use this law by measuring the brightness of the flame within a single photo, we may approximate the temperature profile to also follow an exponential function which decays at a rate 4 times faster than the brightness.

It should be noted in this section that angles greater than 20 degrees yielded very poor results. The flames refused to travel, got stuck on the PLA above it (ruining the channel) or were not able to evaporate enough fuel by the time the next revolution was supposed to start. The same is true for tracks with a diameter smaller than 8cm. As such, accurate measurements were not possible, and the results were discarded.

V. DISCUSSION

As shown in Figure 4, it can be seen that the lifetime of the fuels increases with respect to the opening angle. This makes sense because as the opening gets restricted, less air is able to diffuse into the channel. This restricts the amount of combustion produced and the flames burn colder. This results in the both a smaller concentration of oxidizer, as well as a lower burning temperature, both decreasing the reaction rate found in Equation 2. In this case, the effective length of the opening is $L = L_i \cos\theta$. By compensating the lifetime with an opening of zero degrees by the effective opening size decreasing, as shown in Figure 9 in the appendix, the results correlate strongly to the theoretical fit. In fact, assuming a 20 degree opening, is should be expected that the reaction rate decreases by a factor of 0.94, thereby increasing the lifetime from 38.9 seconds to 41.4 seconds, which is very close to the measured 42.3 seconds lifetime. As such, we believe the mass of evaporated fuel scales linearly with the opening size, as predicted by equation 6.

Furthermore, as Figure 4 demonstrates, the velocity of the flames increases with the radius. This makes sense, as longer tracks mean that each revolution of the flame takes longer. As with the previous explanation, since there is more time for the air to diffuse into the channel and fuel to evaporate, the rate and total enthalpy change of the reaction will be larger, producing more heat, thereby allowing the flame to reach farther neighboring molecules to ignite. Although the rate of evaporation is approximated by an exponential decay, because each revolution is on the order of a few seconds, not enough fuel gets evaporated for us to enter the decaying regime. That said, it should be expected that for much longer tracks (on the length of a meter for example), the best fit of this graph is predicted to be a decaying exponential. Although no model has been found yet, the slope should provide valuable information that can infer on the evaporation rate of the fuel.

Furthermore, in Figure 4, it is found that the velocity of the flame decreases with the angle of the opening. Again, this makes sense because, as explained earlier, the reaction rate and total change in enthalpy are smaller and therefore the fuel burns colder. As such, the flame cannot ignite the fuel as far, decreasing its propagation velocity.

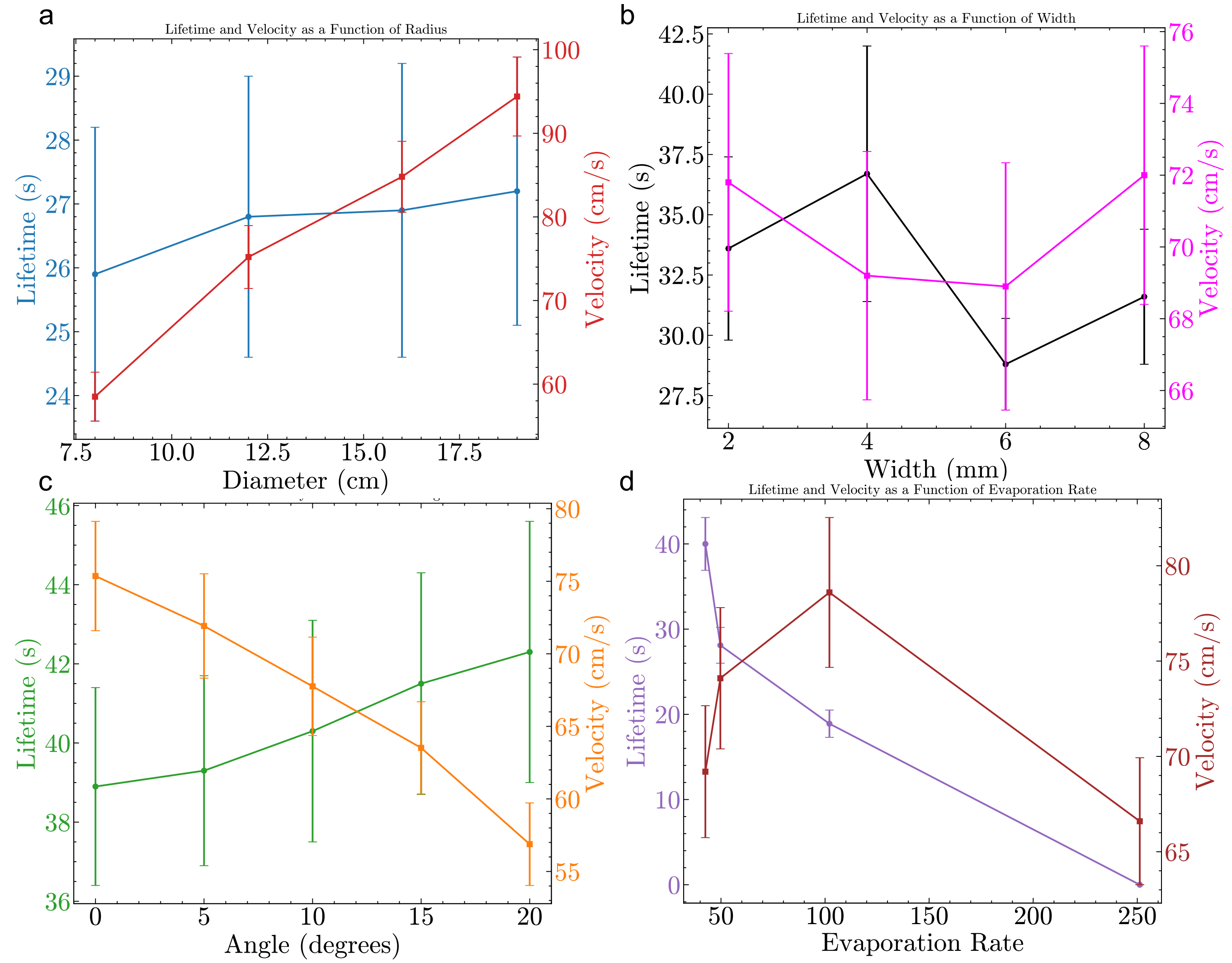

Fig. 4: Plots of all of the main results. For each subplot, the lifetimes and flame velocities per variable are shown. For the relationships with respect to the channel diameter (a), width (b) and angle of opening (c), the fuel used was Zippo lighter fluid. For the relationship with respect to the evaporation rate (d), the various fuel sources as shown in Figure 2 were used. In order of evaporation rate, the fuels were Zippo lighter fluid, IPA, methanol and acetone. Acetone has a lifetime of 0 as all experiments eventually lead to an uncontrolled burn.

Using values from Table I and Equations 1 and 2, theoretical values for laminar flame velocities were computed. These values were found to be 58.2 cm/s for Acetone, 88.7 cm/s for IPA and 97.6 cm/s for Methanol. A theoretical flame speed could not yet be found at the time of writing due to not enough information being available for the fuel and therefore many assumptions having to be taken. However, comparing these values to Fig 4 d), it can be seen that these theoretical values are quite close to the experimental values. Although they are not exactly correct, what is promising and adds credibility to the model is the fact that they are in correct order, the lowest velocity being Acetone and the highest velocity being Methanol.

Similarly, in Figure 4, we measured the effects of varying the width of the channels. That said, as it can be observed, the lifetimes nor the velocity changed in a statistically significant way. It must be noted that the amount of fuel inserted into the channels increased proportionally to the width. This was to be expected, as changing the dimension perpendicular to the direction of travel is not relevant to either of these factors.

Finally, as seen in Figure 4, various fuels provide different lifetimes and velocities. Given that the zippo lighter fluid had the smallest volatility from all the solvents, it had the longest lifetime. Similarly, it released less heat per unit time, thereby decreasing its velocity as explained above. On the other hand, methanol, which burned the quickest, released the most energy per unit time, thereby heating neighboring molecules more and giving it the largest propagation among all the tested fuels! This further solidifies the hypothesis that fuels that burn quicker have larger velocities due to the larger rates of energy they output. It must be noted here that the velocities of the acetone and methyl-acetate mixture where recorded with the camera, as individual flames would be able to travel across the ring. That said, the methyl-acetate mixture had too much water, thereby releasing little fuel vapour. As such, once the flame would make a full revolution, there was not enough vapours collected to restart the reaction. As such, no lifetimes were calculated as the fuel was not fully spent went the flame died. Similarly, acetone, being extremely volatile, would always eventually catch on fire (instead of maintaining individual flame fronts). As such, a lifetime was not possible to be measured.

A basic theoretical estimate was able to be made of the lifetime of the flames when assuming that the evaporation rate of each solvent was it's evaporation rate at 25C. This used the equation $t = \frac{VDM}{EA}$, where V is volume, D density, M molar mass, E evaporation rate, and A area of the ring. This resulted in lifetime estimates of approximately, 165, 2782, 408, and 641 seconds for acetone, IPA, methanol, and the zippo lighter fluid respectively. These are clearly inaccurate to the experimental data. The more sophisticated theoretical model proposed in section III is expected to give a much more accurate result for flame lifetimes — however this has not yet been proven due to the high level of computation required in the sophisticated model. In future exploration of the phenomenon these calculations should be performed by a computer in order to assess the accuracy of the new model.

Smaller channels dipped in a cooling bath to maintain low volatility will be used to attempt to gather a lifetime for all fuels again. All fuels will be tried in this proposed setup for a fair comparison. That said, as outlined by Figure 5 in the appendix, the flames seem to not accelerate over time (nor as the rings heat up), therefore we believe temperature does not have a direct link to the flame velocity.

Additionally, and most interestingly, from Figure 3 Subfirgure 3b the exponential model for the flame front model shows promising initial results. Of the form $300.14 \cdot e^{-0.00198x} + 60.18$, the constant term represents the background noise of the image, the pre-exponential is associated with the flame brightness, whereas the term in the exponent is associated with the velocity and reaction rate of the flame.

Finally, to answer the question of maximizing the lifetime, we see that minimizing the size of the opening of the channel effectively minimizes the evaporation rate of the fuel. Furthermore, rings with larger diameters mean that the average temperature of the fuel is colder. As such, the total volume of evaporated fuel per cycle is smaller. As for the choice of fuel, Zippo lighter fluid, the one with the smallest evaporation rate, was the best case. Given that it was difficult to kickstart a flame reaction, we believe that fuels with smaller evaporation rates (as demonstrated by the methyl-acetate and water mixture) will not be able to support a reaction. Furthermore, we do not believe that there is any theoretical explanation or experimental support to the channel width changing the lifetime.

VI. CONCLUSION

This report successfully demonstrates the theoretical modelling and experimental observations in understanding travelling flames in ring-shaped channels. The report highlights the critical influence of fuel properties, channel geometry, and opening angles on flame dynamics. Theoretical equations, particularly those governing laminar flame speed and reaction rates, provided a robust framework for interpreting the experimental data. Key findings include the proportional relationship between channel size and flame velocity, the dependence of flame lifetime on fuel volatility, and the validation of exponential decay models for flame characteristics. The methodology, involving 3D-printed channels and high-resolution imaging, proved effective in capturing and analyzing flame behaviour. Future work could explore longer channels, additional fuels, and asymmetric geometries to further refine the models.

Furthermore, the ability to use the theoretical models to cross-verify the results is imperative and will be further refined to decrease the disparities between the theoretical predictions and experimental results (especially in the lifetime predictions). Finally, to maximize the lifetime of a given flame, a long channel with 0.2ml of fuel (with an evaporation rate of around $35 \frac{mg}{m^2 s}$) per 37cm of length and channel opening of 20 degrees should be used. A potential improvement to further lengthen the lifetime is to use a channel that sits on a heat sink or cold surface to keep the temperature and evaporation rate low.

REFERENCES

[1] Acetone - Thermophysical Properties — engineeringtoolbox.com. https://www.engineeringtoolbox.com/acetone-2-propanone-dimethyl-ketone-properties-d_2036.html. [Accessed 24-01-2025].

[2] Adiabatic flame temperature - Wikipedia — en.wikipedia.org. https://en.wikipedia.org/wiki/Adiabatic_flame_temperature. [Accessed 24-01-2025].

[3] Isopropyl Alcohol — webbook.nist.gov. https://webbook.nist.gov/cgi/cbook.cgi?ID=C67630&Mask=4. [Accessed 24-01-2025].

[4] Methanol - Thermophysical Properties — engineeringtoolbox.com. https://www.engineeringtoolbox.com/methanol-methyl-alcohol-properties-CH3OH-d_2031.html. [Accessed 24-01-2025].

[5] Molecular Flux Provides Process Understanding — normandale.edu. https://www.normandale.edu/academics/degrees-certificates/vacuum-and-thin-film-technology/articles/molecular-flux-provides-process-understanding.html#:~:text=We%20can%20easily%20calculate%20the,%2C%20and%20T%20=%20ÂřK. [Accessed 24-01-2025].

[6] n-Hexane — webbook.nist.gov. https://webbook.nist.gov/cgi/cbook.cgi?ID=C110543&Mask=2269. [Accessed 24-01-2025].

[7] Testing the Thermal Conductivity of Solvents — thermtest.com. https://thermtest.com/application/thermal-conductivity-solvents. [Accessed 24-01-2025].

[8] Chapter 7 - process safety and pressure-relieving devices. In *Emphasizes how to apply techniques of process design and interpret results into mechanical equipment details*, E. E. Ludwig, Ed., vol. 1 of *Applied Process Design for Chemical Petrochemical Plants*. Gulf Professional Publishing, 1999, pp. 399–546.

[9] D. G. KLISSURSKI, E. F. MCCAFFREY, R. A. R. The Catalytic Decomposition of Isopropyl Alcohol Vapor on Manganese (II) Oxide. https://cdnsciencepub.com/doi/10.1139/v71-631. [Accessed 23-01-2025].

[10] DAVIDZON, M. I. Newton's law of cooling and its interpretation. *International Journal of Heat and Mass Transfer 55*, 21 (2012), 5397–5402.

[11] FARTUX. Oxygen Not Included Database — oni-db.com. https://oni-db.com/details/naphtha. [Accessed 24-01-2025].

[12] HAEMMERICH, D. 1 - mathematical modeling of heat transfer in biological tissues (bioheat transfer). In *Principles and Technologies for Electromagnetic Energy Based Therapies*, P. Prakash and G. Srimathveeravalli, Eds. Academic Press, 2022, pp. 1–24.

[13] RIBBING, C. 8 - controlling thermal radiation from surfaces. In *Optical Thin Films and Coatings*, A. Piegari and F. Flory, Eds., Woodhead Publishing Series in Electronic and Optical Materials. Woodhead Publishing, 2013, pp. 357–390.

[14] ZAMARRIPA, M., HJAILA, K., SILVENTE, J., AND ESPUÑA, A. Simplified model for integrated supply chains planning. In *23rd European Symposium on Computer Aided Process Engineering*, A. Kraslawski and I. Turunen, Eds., vol. 32 of *Computer Aided Chemical Engineering*. Elsevier, 2013, pp. 547–552.

[15] ZELDOWITSCH, J., AND FRANK-KAMENETZKI, D. A theory of thermal propagation of flame. In *Dynamics of Curved Fronts*, P. Pelcé, Ed. Academic Press, San Diego, 1988, pp. 131–140.

.

APPENDIX

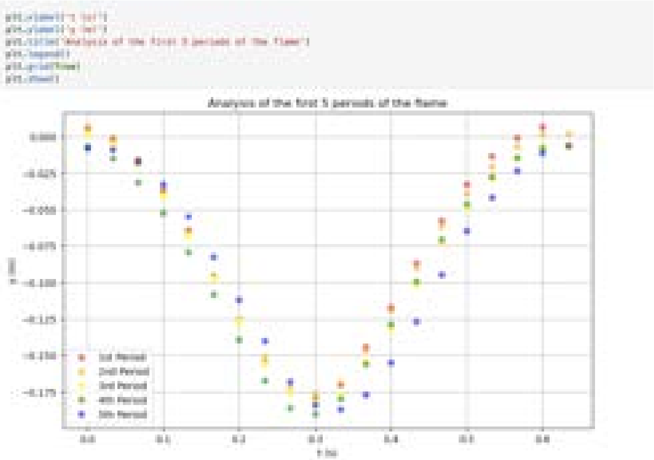

Fig. 5: Graph of the vertical position of a flame over time. This graph is used to demonstrate that the flame does not experience significant acceleration over time.

Equation for the CDF of the Boltzmann distribution

$$\sigma(T) = \frac{1-\operatorname{erf}\left(\frac{v}{\sqrt{2}\left(\sqrt{k\cdot\frac{T(x)}{m}}\right)}\right)+\sqrt{\frac{2}{\pi}}\left(\frac{v}{\left(\sqrt{k\cdot\frac{T(x)}{m}}\right)}\right)\exp\left(-\frac{v^2}{2\left(\sqrt{k\cdot\frac{T(x)}{m}}\right)^2}\right)}{1-\left(\operatorname{erf}\left(\frac{v}{\sqrt{2}\left(\sqrt{k\cdot\frac{298}{m}}\right)}\right)-\sqrt{\frac{2}{\pi}}\left(\frac{v}{\sqrt{k\cdot\frac{298}{m}}}\right)\exp\left(-\frac{v^2}{2\left(\sqrt{k\cdot\frac{298}{m}}\right)^2}\right)\right)} \tag{9}$$

Here, v is the minimum velocity of the molecules required to overcome the enthalpy of evaporation of the fuel, k is Boltzmann's constant, m is the mass of the molecule and T(x) is the Temperature of the fuel across the length of the channel.

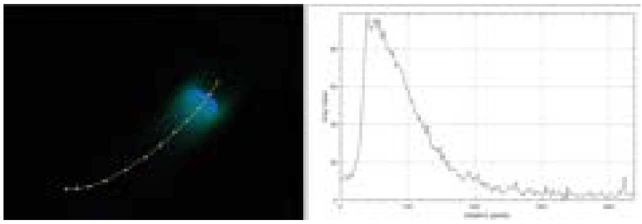

Fig. 6: Image as well as a graph with a line profile of the flame front brightness. In contrast with a similar figure above, here a section in front of the flame is shown, demonstrating how "sharp" the flame-front is.

	Acetone	**Isopropyl Alcohol**	**Methanol**	**Zippo Lighter Fluid**
Thermal Conductivity (W/m °C)	0.18	0.137	0.202	0.2
Density (mol/m^3)	13507	43371	24540	7003
Specific Heat (J/mol K)	75	89	116	2.191
Evaporation Rate (mg/ m^2 s^1)	251.2	49.7	102.1	42.5
Molar mass (g/mol)	58.08	60.1	32.04	102.2
Vapor Pressure (Pa)	30664.1	6053	16933	4000
Temperature of Flame (°C)	1980	1926	1949	2533
Autoignition Temperature (°C)	465	399	470	265
m	1	1	2	2
n	4	2	3	19
Activation Energy (Ea) (KJ/mol)	67.86	108.784	43	121.6
Heat Enthalpy of Evaporation (ΔH) (KJ/mol)	31.0	37.34	44.0	28.9
Mass of molecule (g)	9.645 x 10^{-23}	9.980 x 10^{-23}	5.230 x 10^{-23}	1.697 x 10^{-22}

TABLE I: Theoretical vales for parameters for the different fuels used. These values can be used in comparison to experimental values. [1], [4], [3], [6], [2], [9], [11], [5], [7]

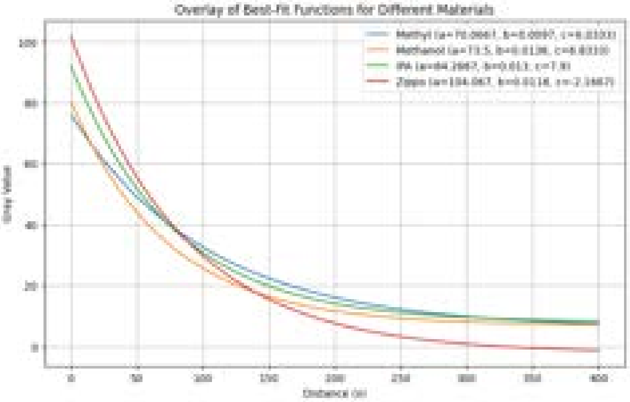

Fig. 7: Graph showing the best fits of the flame front equations for Methyl Acetate, Methanol, IPA and Zippo lighter fuel. It can be appreciated that all fuels do not change drastically in their characteristics.

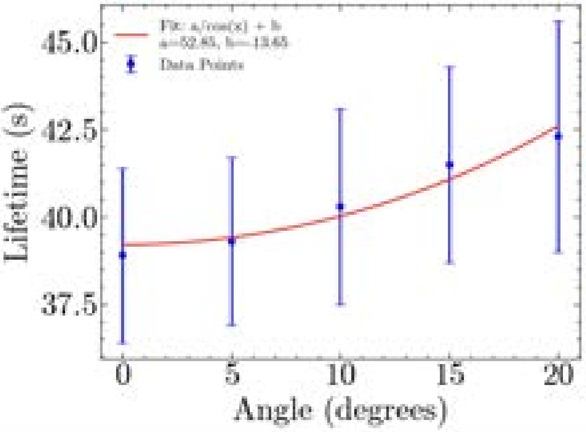

Fig. 8: Evaporation rate of the fuel with respect to the angle of opening. Note the best-fit line closely follows the evaporation rate, demonstrating how the trigonometric behaviour of the effective opening size determines the lifetime.

Methanol: $2\,CH_3OH\,(g) + 3\,O_2(g) \longrightarrow 2\,CO_2\,(g) + 4\,H_2O\,(g)$
Acetone: $C_3H_6O\,(g) + 4\,O_2(g) \longrightarrow 3\,CO_2\,(g) + 3\,H_2O\,(g)$
Isopropyl Alcohol: $2\,C_3H_8O\,(g) + 9\,O_2(g) \longrightarrow 6\,CO_2\,(g) + 8\,H_2O\,(g)$

Fig. 9: Chemical reactions for the combustion of Methanol, Acetone, and Isopropyl Alcohol.